A Density Functional Study on the Stereocontrol of the Sharpless Epoxidation

Yun-Dong Wu* and David K. W. Lai

Contribution from the Department of Chemistry, Hong Kong University of Science and Technology, Clear Water Bay, Kowloon, Hong Kong

Received January 12, 1995[⊗]

Abstract: Density functional calculations have been carried out to model the dimeric mechanism of the Sharpless epoxidation. A hexacoordinated system Ti(O−CH_2−CH_2−O)(O−O−Me)(O−CH_2−CH=CH_2)(H_2O) (**10**) was first studied in detail. Transition structures were fully optimized with the nonlocal density functional approximation (BLYP) and the 3-21G basis set. Energies were further calculated with the HW3 basis set (equivalent to the 6-31G* basis set). The calculated activation energy is close to those observed experimentally. The titanium center in each transition structure has a distorted octahedral geometry. The Ti−O−O unit has a perfect η^2 structure. The Ti−O−O approaches the C=C in a spiro fashion with the two C- - -O bonds forming to similar extents. There is a significant conformational preference for the peroxy alkoxy group to be away from the bridging oxygen. The allylic alcohol substrate strongly favors a conformation with the allylic C−O bond gauche to the Ti−O_{water} bond if the oxidant is *tert*-butyl peroxide. This conformational preference vanishes if the oxidant is methyl hydroperoxide. The tartrate ester groups were modeled with formyl groups and were found to favor equatorial conformation instead of axial conformation in the transition structure. A modified Sharpless dimeric model is developed which uniquely explains the importance of the bulky peroxide and ligand structure to the stereochemistry of the Sharpless epoxidation.

In 1980, Sharpless *et al.* achieved a breakthrough in enantioselective epoxidation of allylic alcohols.[1] They showed that in the presence of *tert*-butyl hydroperoxide (TBHP), titanium (IV) catalyst, and a chiral tartrate ligand, an allylic alcohol can be converted into epoxides with good yield and with excellent enantioselectivity. In the following years, the reaction was improved to give excellent results for almost all types of allylic alcohols except for a few special cases.[2,3] This reaction is now referred to as the Sharpless epoxidation. As shown in Figure 1, the chiral ligand is critical to the enantioselectivity.[2a] Thus, both tartrate esters and secondary tartaric amides give high enantioselectivity (entries 1 and 2). Primary tartaric amide (entry 3), however, gives poor enantioselectivity. If one of the tartaric ester groups is replaced by a sterically bulky group (entries 4 and 5), high enantioselectivity can still be achieved. But if both the ester groups are replaced by phenyl or methyl groups (entries 7 and 8), the stereoselectivity is lost. Entries 10−12 indicate the importance of the positions of the glycolate and ester groups.[4]

The bulkiness of the oxidant is also important to the stereochemistry.[5] *tert*-Butyl hydroperoxide and triphenylmethyl hydroperoxide (trityl) generally lead to high stereoselectivities but primary hydrogen peroxides give much lower stereoselectivity.[5,6] For example, epoxidation with stoichiometric titanium tartrate and *n*-butyl hydroperoxide of (*E*)-2-decen-1-ol affords epoxy alcohol of about 75% ee while trityl and *tert*-butyl hydroperoxides each provide >95% enantioselectivity excess under identical conditions.[6]

Besides the high enantioselectivity for prochiral allylic alcohols, this reaction is also sensitive to the chiral environment in the allylic alcohol. Thus, when a racemic mixture of α-chiral allylic alcohol is used as substrate, highly efficient kinetic resolution can be achieved. The mode of diastereoselectivity is also predictable. However, the alkoxide ligands have some important influences on the diastereoselectivity.[2] McKee *et al.* found that when *tert*-butyl alcohol is used instead of isopropyl alcohol, the kinetic resolution efficiency is reduced.[7a]

Originally, Sharpless *et al.* proposed a dimeric mechanism with a ten-membered ring and a pentacoordinate transition state (**1**) for asymmetric epoxidation,[8] based on the finding of an X-ray crystal structure of the related analog complex of vanadium(IV) with tartaric acid.[9] This mechanism has been further discussed recently by Potvin[10] and Erker.[11] However, X-ray crystal structures of several related titanium tartrate

[⊗] Abstract published in *Advance ACS Abstracts*, November 1, 1995.

(1) Katsuki, T.; Sharpless, K. B. *J. Am. Chem. Soc.* **1980**, *102*, 5974.

(2) For excellent reviews on the topic, see: (a) Finn, M. G.; Sharpless, K. B. In *Asymmetric Synthesis*; Morrison, J. D., Ed.; Academic Press: New York, 1986; Vol. 5, p 247. (b) Rossiter, B. E. In *Asymmetric Synthesis*; Morrison, J. D., Ed.; Academic Press: New York, 1986; Vol. 5, p 193. (c) Johnson, R. A.; Sharpless, K. B. In *Comprehensive Organic Synthesis*; Trost, B. M., Ed.; Pergamon Press: New York, 1991; Vol. 7, Charper 3.2.

(3) (a) Rossiter, B. E.; Katsuki, T.; Sharpless, K. B. *J. Am. Chem. Soc.* **1981**, *103*, 464. (b) Martin, V. S.; Woodard, S. S.; Katsuki, T.; Yamada, Y.; Ikeda, M.; Sharpless, K. B. *J. Am. Chem. Soc.* **1981**, *103*, 6237. (c) Gonnella, N. C.; Nakanishi, K.; Martin, V. S.; Sharpless, K. B. *J. Am. Chem. Soc.* **1982**, *104*, 3775. (d) Hill, J. G.; Rossiter, B. E.; Sharpless, K. B. *J. Org. Chem.* **1983**, *48*, 3607. (e) Hanson, R. M.; Sharpless, K. B. *J. Org. Chem.* **1986**, *51*, 1922.

(4) Burns, C. J.; Martin, C. A.; Sharpless, K. B. *J. Org. Chem.* **1989**, *54*, 2826.

(5) Gao, Y.; Hanson, R. M.; Klunder, J. M.; Ko, S. Y.; Masamune, H.; Sharpless, K. B. *J. Am. Chem. Soc.* **1987**, *109*, 5765.

(6) Woodard, S. S.; Finn, M. G.; Sharpless, K. B. *J. Am. Chem. Soc.* **1991**, *113*, 106.

(7) (a) McKee, B. H.; Kalantar, T. H.; Sharpless, K. B. *J. Org. Chem.* **1991**, *56*, 6966. (b) Carlier, P. R.; Mungall, W. S.; Schroder, G.; Sharpless, K. B. *J. Am. Chem. Soc.* **1988**, *110*, 2978. (c) Carlier, P. R.; Sharpless, K. B. *J. Org. Chem.* **1989**, *56*, 6966.

(8) Sharpless, K. B.; Woodard, S. S.; Finn, M. G. *Pure Appl. Chem.* **1983**, *55*, 1823.

(9) (a) Hahs, S. K.; Ortega, R. B.; Tapscott, R. E.; Campana, C. F.; Morosin, B. *Inorg. Chem.* **1982**, *21*, 664. (b) Tapscott, R. E.; Robbins, G. L. *Inorg. Chem.* **1976**, *15*, 154. (c) Tapscott, R. E.; Belford, R. L.; Paul, I. C. *Coord. Chem. Rev.* **1969**, *4*, 323.

(10) (a) Potvin, P. G.; Bianchet, S. *J. Org. Chem.* **1992**, *57*, 6629. (b) Potvin, P. G.; Kwong, P. C. C.; Brook, M. A. *J. Chem. Soc.* **1988**, 773. (c) Potvin, P. G.; Kwong, P. C. C.; Gau, R.; Bianchet, S. *Can. J. Chem.* **1989**, *67*, 1523.

(11) (a) Erker, G.; Dehnicke, S.; Rump, M.; Krüger, C.; Werner, S.; Nolte, M. *Angew. Chem., Int. Ed. Engl.* **1991**, *30*, 1349. (b) Erker, G.; Noe, R. *J. Chem. Soc., Dalton Trans.* **1991**, 685.

0002-7863/95/1517-11327$09.00/0

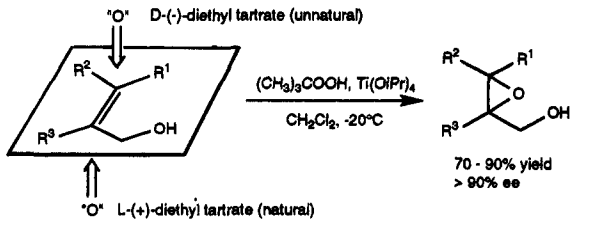

entry		%ee	entry		%ee
1	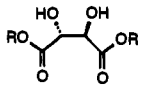	>98 (S)	7	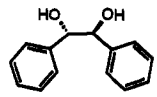	0
2	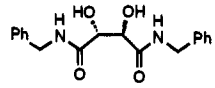	96 (S)	8		5 (R)
3	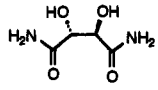	19 (R)	9		13 (S)
4	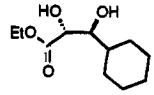	>98 (S)	10	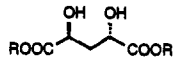	95(R)
5	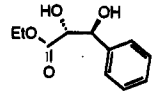	80 (S)	11	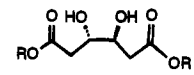	0
6	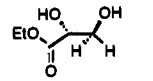	35 (S)	12	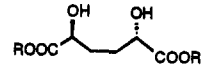	28(R)

Figure 1. Scheme for the Sharpless epoxidation and selected examples of chiral ligand dependence of the enantioselectivity of epoxidation of 2,3-diphenylbutanol.

complexes all exist in dimeric forms with two Ti−O−Ti bridges.[12] Consequently, IR, ^{1}H, ^{13}C, and ^{17}O NMR spectrometries in conjunction with the Signer method of molecular weight measurements also suggest that the active catalyst is in a dimeric form in solution.[13] A monomeric titanium tartrate complex has not been detected. Therefore, Sharpless *et al.* proposed a dimeric hexacoordinate transition state model (**2**) which also qualitatively explains the observed stereoselectivity.[2a,12a] The detailed formulation of the model can be found in ref 2a. While the mode of allylic alcohol loading is uncertain (top or bottom),[14] the model explains the observed enantioselectivity and diastereoselectivity based on steric arguments. For example, in structure **2**, the allylic C−O favors gauche to the non-bridging $Ti-O_{diolate}$ bond. This structure leads to the formation of the major enantiomeric product. If the allylic C=C approaches the peroxide from the other face, the allylic C−O bond would have to be gauche to the $Ti-O_{bridging}$ bond. This transition structure would suffer from steric interaction with the non-coordinate ester group in the bystander portion of the dimer. Thus, the enantioselectivity is determined by the chirality of the chiral tartrate ligand. This model also predicts the diastereoselectivity. When the α-center of the allylic alcohol is chiral, the two enantiomeric substrates have R2 = alkyl and R3 = alkyl, respectively. It is obvious that the enantiomer with R2 = alkyl suffers from more steric interaction in structure **2** and, therefore, undergoes epoxidation more slowly than the other enantiomer.

Recently, Corey proposed an ion-pair mechanism in which the transition state adopts a monomeric and pentacoordinated complex which is in a square-pyramidal geometry (**3**) to explain the stereoselectivity of the Sharpless epoxidation.[15] The ion-pair model is derived from the dissociation of the dimeric hexacoordinated complex with the addition of an allylic alcohol and an alkyl hydroperoxide. The key feature of the model is the hydrogen bonding between the allylic alcohol and the ester group which is suggested to determine the arrangement of the allylic alcohol.

Finn and Sharpless noted that the Corey monomeric mechanism does not obey the kinetics of the epoxidation reaction.[13] With pseudo-first-order kinetic experiments, the rate law is expressed in eq 1.[6]

$$\text{rate} = k\frac{[\text{Ti(tartrate)(OR)}_2][\text{TBHP}][\text{allylic alcohol}]}{[\text{inhibitor alcohol}]^2} \quad (1)$$

The fact that the rate is inversely proportional to the square of the inhibitor alcohol concentration indicates that two alcohol molecules are released from the titanium catalyst during the epoxidation. In the Corey mechanism, no alcohol is released. In addition, the above rate law is not changed over a 10-fold range of starting concentration of [Ti(OR)$_2$(tartrate)], which is also difficult to reconcile with the Corey model. It is also difficult to explain the observation that the kinetic resolution efficiency is dependent on the structure of alkoxide ligand based on a monomeric mechanism.[7]

Jørgensen, Wheeler, and Hoffmann reported extended Hückel molecular orbital calculations for the structure and epoxidation properties of titanium tartrate asymmetric epoxidation.[16] They suggested a dimeric preference of the reaction, analyzed the coordination of peroxide to titanium tartrate which favors an equatorial peroxygen, and found a large preference for a spiro epoxidation transition state over a planar transition state.[16] In particular, they identified two favorable orientations of the allylic alcohol moiety which allow a spiro epoxidation transition state. These are schematically shown by **4** and **5**. According to calcultions, structure **4** should be much more stable than **5**. Besides a possible steric destabilization in **5** between the allyl moiety and the tartrate ester group, they proposed that **4** is stabilized by an electrostatic attraction between the allylic oxygen lone pair and the partially positively charged carbonyl carbon, which is absent in structure **5**. The preference for **4** over **5** is also in accord with the observed enantioselectivity. According to this model, the axial orientation of the two tartrate ester groups is essential to the high enantioselectivity since both the steric effect and the electrostatic effect can be achieved only when the ester groups are axially oriented.

Detailed information regarding the geometrical features and energetics of the transition states of titanium tartrate complex mediated epoxidations will facilitate understanding of both the mechanism and the stereocontrol of the reaction. In 1984 Bach *et al.* analyzed the molecular orbitals of metal hydroperoxide and explained the electrophilic nature of epoxidation and the role of metal catalysis.[17] For the model reaction of Li−OOH with ethylene, they found that a spiro transition state (**6**) is more stable than a planar one (**7**) by about 1 kcal/mol.[17] The spiro preference of the transition state of metal-catalyzed epoxidation

(12) (a) Willians, I. D.; Pedersen, S. F.; Sharpless, K. B.; Lippard, S. J. *J. Am. Chem. Soc.* **1984**, *106*, 6430. (b) Pedersen, S. F.; Dewan, J. C.; Eckman, R. R.; Sharpless, K. B. *J. Am. Chem. Soc.* **1987**, *109*, 1279.

(13) Finn, M. G.; Sharpless, K. B. *J. Am. Chem. Soc.* **1991**, *113*, 113.

(14) While the top loading of allylic alcohol was originally proposed, subsequent publications have featured bottom loading of the allylic alcohol.

(15) Corey, E. J. *J. Org. Chem.* **1990**, *55*, 1693.

(16) Jørgensen, K. A.; Wheeler, R. A.; Hoffmann, R. *J. Am. Chem. Soc.* **1987**, *109*, 3240.

(17) Bach, R. D.; Wolber, G. J.; Coddens, B. A. *J. Am. Chem. Soc.* **1984**, 106, 6098.

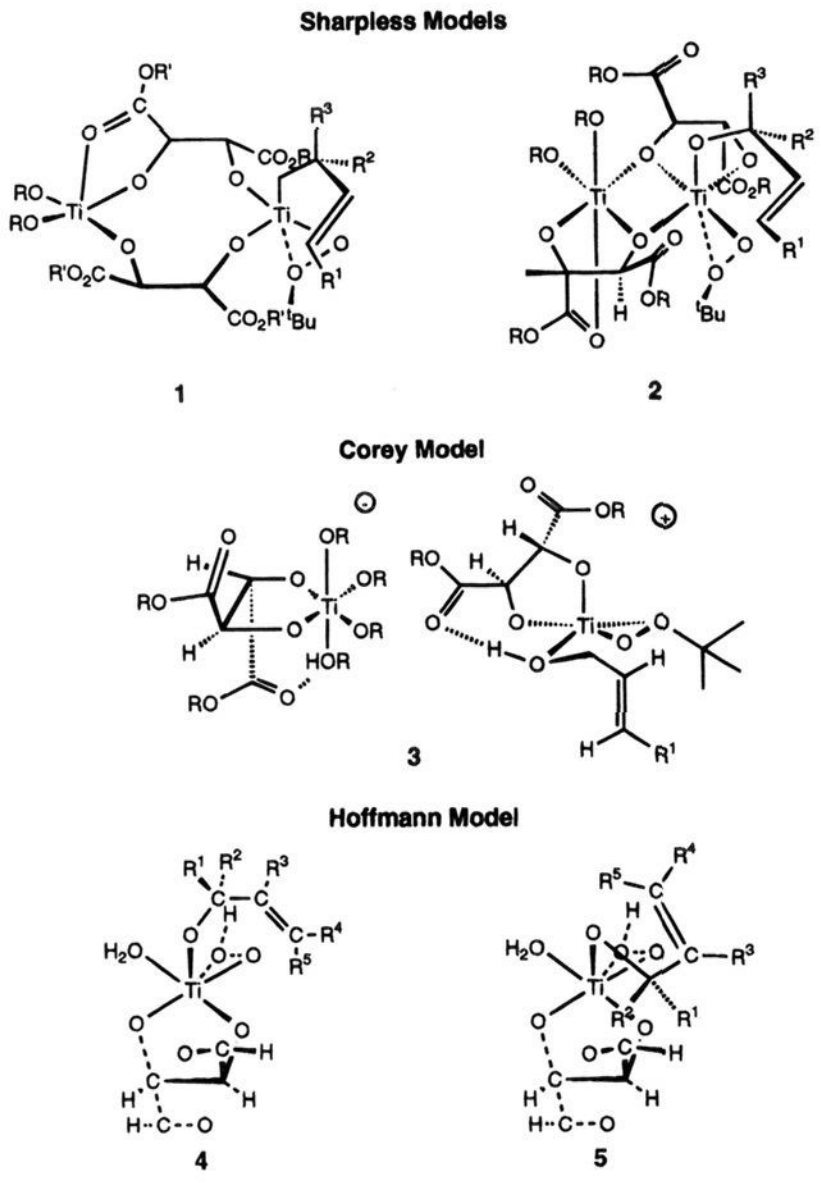

Figure 2. Schematic representations of proposed models for the stereocontrol of the Sharpless epoxidation. In **2**, the stereoselectivity is controlled by steric interaction. In **3**, the key is the hydrogen bond.

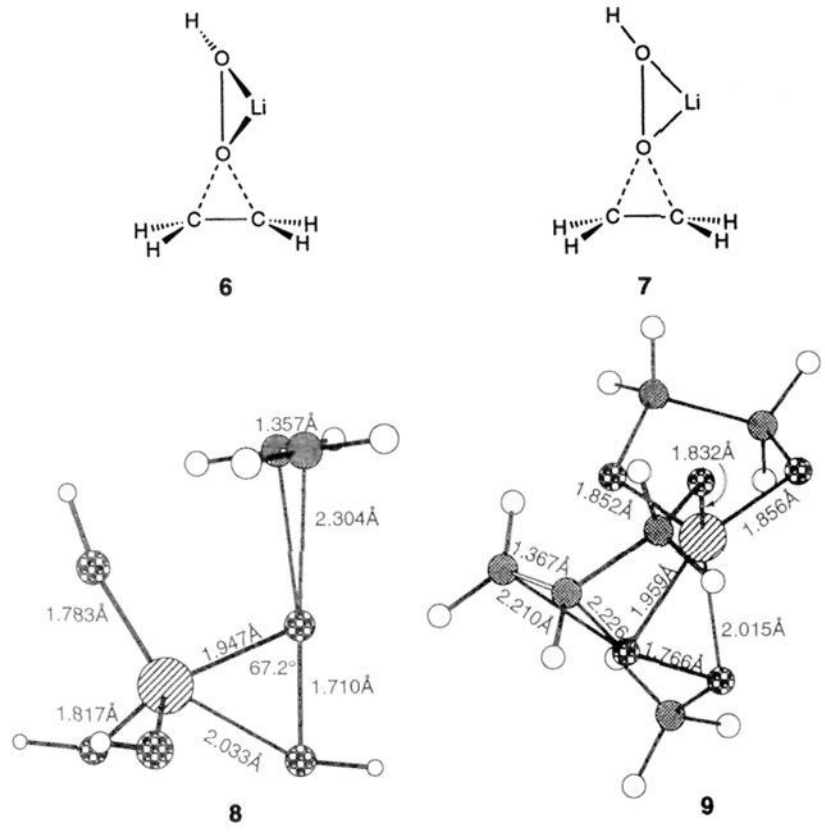

was also found by Jørgensen *et al.* in the extended Hückel molecular orbital study of the Sharpless epoxidation.[16] Recently, we reported a high-quality density functional study of the transition structures (or transition state structures) of titanium-catalyzed epoxidations. For an acyclic model, we found a spiro transition structure (**8**) to be more stable than a planar one by about 3 kcal/mol. For a cyclic pentacoordinate system only spiro transition structures such as **9** could be found.[18] Since

(18) Wu, Y.-D.; Lai, D. K. W. *J. Org. Chem.* **1995**, *60*, 673.

Scheme 1

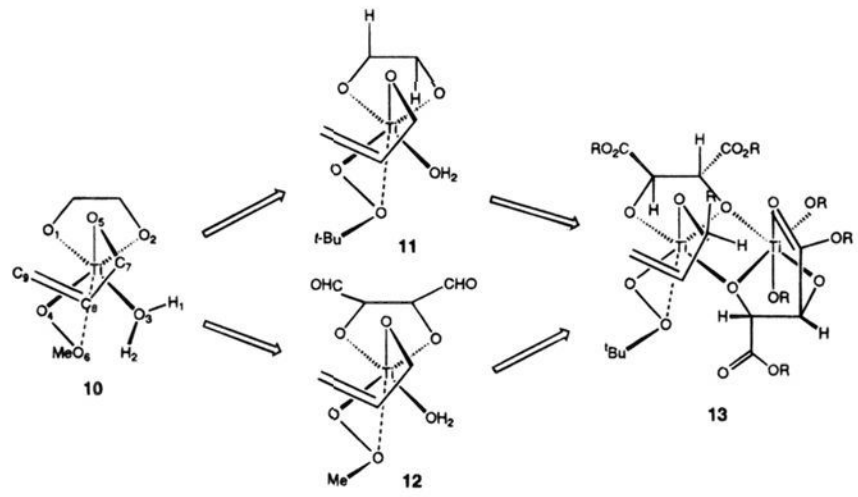

full geometric optimizations were carried out, many geometrical features of the transition structure of titanium-mediated epoxidation were revealed.

In this paper, we report a density functional study of the transition structures of Ti-catalyzed epoxidation of allylic alcohol which mimics the dimeric mechanism proposed by Sharpless *et al.* In particular, we address the importance of the bulkiness of alkyl hydroperoxide to the stereoselectivity, the conformational features of tartrate esters in the epoxidation transition structure, and the loading of allylic alcohol in the dimeric transition structure model.

Method of Calculation

Density functional calculations have been carried out by the Gaussian 92/DFT program,[19] using the BLYP non-local density functional approximation, which uses Becke's 88 non-local exchange functional[20] and the Lee-Yang-Parr non-local correlation functional.[21] This method has been shown to give quite good results for many systems,[22] including transition structures.[23] Geometric optimizations were carried out with the 3-21G basis set first.[24] It has been shown that this basis set gives quite satisfactory geometries of transition structures.[18] Energy evaluations were done according to Frenking[25] with the HW3 basis set, which was constructed by contraction scheme [3311/2111/311] + ECP on a 10 electron core for the titanium atom and the 6-31G* basis set for other atoms. Therefore, this basis set is equivalent to the 6-31G* basis set. Strategy of the Research

Strategy of the Research

The strategy of our theoretical study is outlined in Scheme 1. In the first stage a relatively simple system (**10**) was studied in detail with the full optimization of eight transition structures. This model excluded the bystander titanium center. The two tartrate ester groups were also not calculated. The oxidant was methyl peroxide. A water molecule was added to model the bridging oxygen from the second titanium center so that the reactive titanium center is in a hexacoordination environment. A geometry constraint was imposed on all calculations. The bond angles $\angle H_1-O_3-Ti$ and $\angle H_2-O_3-Ti$ of the two hydrogen atoms in the H_2O moiety were fixed at 114.5° and 128.4°, respectively; the former is close to that of the Ti−O−Ti angle in crystal

(19) Gaussian 92/DFT Revision F.2; Frisch, M. J.; Trucks, G. W.; Schlegel, H. B.; Gill, P. M. W.; Johnson, B. G.; Wong, M. W.; Gomperts, R.; Andres, J. L.; Raghavachari, K.; Binkley, J. S.; Gonzalez, C.; Martin, R. L.; Fox, D. J.; Defrees, D. J.; Baker, J.; Stewart, J. J. P.; Pople, J. A. Gaussian, Inc.: Pittsburgh, PA, 1993.

(20) Becke, A. D. *Phys. Rev.* **1988**, *A38*, 3098.

(21) Lee, C.; Yang, W.; Parr, R. G. *Phys. Rev.* **1988**, *B37*, 785.

(22) Johnson, B. G.; Gill, P. M. W.; Pople, J. A. *J. Chem. Phys.* **1993**, *98*, 5612.

(23) (a) Ziegler, T. *Chem. Rev.* **1991**, *91*, 651. (b) Fan, L.; Ziegler, T. *J. Am. Chem. Soc.* **1992**, *114*, 10890. (c) Stanton, R. V.; Merz, K. M., Jr. *J. Chem. Phys.* **1994**, *100*(1), 434.

(24) Dobbs, K. D.; Hehre, W. J. *J. Comput. Chem.* **1987**, *8*, 861.

(25) (a) Jonas, V.; Frenking, G.; Reetz, M. T. *J. Comput. Chem.* **1992**, *13*, 919. (b) Jonas, V.; Frenking, G.; Reetz, M. T. *Organometallic* **1993**, *12*, 2111. (c) Hay, P. J.; Wadt, W. R. *J. Chem. Phys.* **1985,** *82*, 299.

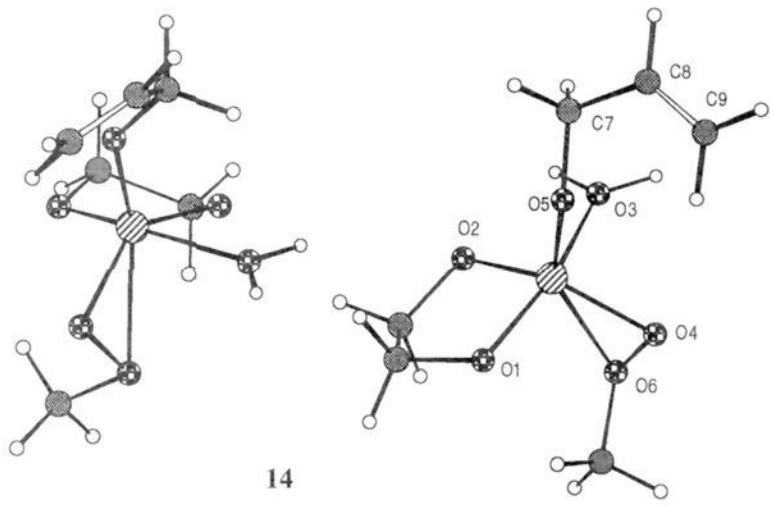

Figure 3. Two views of the optimized reactant of model **10**.

structures of titanium tartrate complexes.[12] The two dihedral angles $\angle H_1-O_3-Ti-O_2$ and $\angle H_2-O_3-Ti-O_2$ between the hydrogen atoms in the H_2O moiety and the diolate oxygen anti to the peroxygen were also accidentally fixed at 7.6° and −169.0° for all structures. The more proper values would be 0° and 180° to better mimic the planar Ti_2O_2 unit in the X-ray structures of titanium tartrate complexes.[12] We also optimized structures **15** and **16** with the 0° and 180° constraints and found essentially no geometrical change (*vide infra*). The geometry constraint is necessary in order to prevent hydrogen bonding between the hydrogen and the diolate oxygen, or the hydrogen and the peroxo oxygen nearby. Such hydrogen bonding would cause undesirable structural distortion such that H_2O would no longer be the model to mimic the bridged diolate oxygen.

In the second stage, the effect of bulkiness of peroxide was studied with *tert*-butyl peroxide as the oxidant (**11**). The conformational features of tartrate ester groups were studied by the addition of two formyl groups to the most favorable conformations for **10**. After these studies, we formulated a dimeric model (**13**) which is somewhat different from that proposed by Sharpless to rationalize the stereoselectivity of the Sharpless epoxidation.

Results and Discussion

A. The Reactant of Model 10. For model **10**, the reactant was first optimized. This served as a reference for the calculation of activation energy. Two views of the optimized structure are shown in Figure 3. It should be pointed out that no vigorous search for a most stable conformation was performed. However, it is unlikely that a much more stable conformation will be found. This structure leads to transition structure **19**, as shown in Figure 4, upon approach of the C=C double bond to the peroxy oxygen without other significant conformational change. The C=C−C−O dihedral angle is near 0°. This conformation is in agreement with the preferred conformation of allylic alcohol and allylic ethers studied by experiment.[26] Structure **14** is close to a square-pyramidal structure, with the allylic oxygen ligand axial. The $Ti-O_4-O_6(Me)$ unit can be regarded as an unsymmetrical η^2 structure because the $Ti-O_4-O_6$ angle is only about 82° and the $Ti-O_5$ and $Ti-O_6$ distances are 1.8 and 2.3 Å, respectively. These are similar to the results reported by Boche *et al.*[27] and Jørgensen[28] on simpler Ti−OOH complexes. The allylic C−O bond in structure **14** is gauche to the $Ti-O_3$ and $Ti-O_4$ bonds. The C=C double bond is far away from the electrophilic peroxygen (C- -O distances = 4.239, 4.597 Å). The five-membered diolate ring is in an expected half-chair conformation with two C−H bonds nearly axial (>H−C−C−H =167°) and

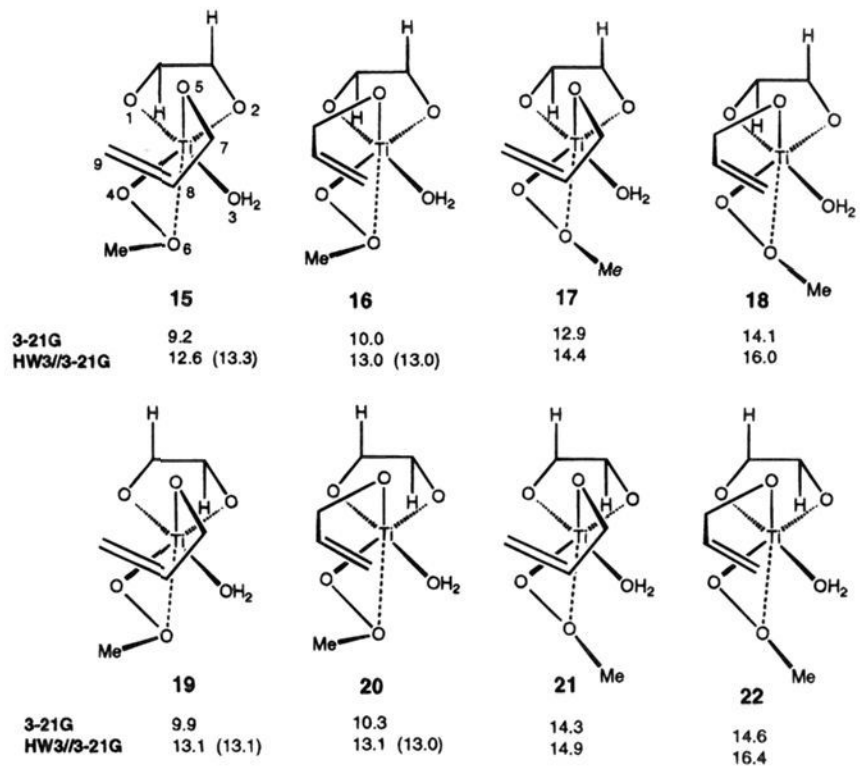

Figure 4. The schematic drawings and calculated activation energies (kcal/mol) of the eight possible transition structures with respect to structure **14**. The atomic numbering is given in **15**. The values in parentheses are calculated with the rotation of the H1−O3−Ti−O2 and H2−O3−Ti−O2 dihedral angles to 0° and 180°, respectively (see text).

the other two C−H bonds nearly equatorial (>H−C−C−H = 77°). The O_1-Ti-O_2 angle is about 84°, somewhat larger than the corresponding one in the crystal structure of titanium tartrate complex.[12] The O_1-Ti-O_4 angle is about 30° larger than the O_2-Ti-O_3 angle, reflecting the much weaker coordination of water. Interestingly the calculated O_2-Ti-O_3 angle is about 74°, close to the angle involving the two bridging oxygens in the crystal structure of titanium tartrate complex.[12] It has been noted that the Ti−O−alkyl angle is quite large in the X-ray crystal structures of d^0 metal alkoxide systems.[12] This is often attributed to p_n-d back-donation.[29] The natural population analysis[30] supports this explanation. The Ti(IV) has a net positive charge of 1.627 units. There is significant electron occupation in the metal 3d atomic orbitals. However, the geometrical feature can also be explained by electrostatic interactions.[31] The Ti atom is very positively charged, and has attractive interaction with the hydroxy lone pairs. The large basis set dependence of the Ti−O−H angles supports such an explanation. The calculated O−O bond length is 1.493 Å, which is comparable to those determined by both high-level *ab initio* calculations[32] and experiments.[33]

B. Transition Structures of Model 10. As shown in Figure 4, there are eight possible transition structures for model **10**. Besides the two possible conformations for the allyl moiety, the methyl group of the alkyl peroxide can also adopt two

(26) (a) Murty, A. N.; Curl, R. F., Jr. *J. Chem. Phys.* **1967**, *46*, 4176. (b) Brown, R. S.; Marcinko, R. W. *J. Am. Chem. Soc.* **1978**, *100*, 5721. (c) Silvi, B.; Froment, F.; Corset, J.; Perchard, J. P. *Chem. Phys. Lett.* **1973**, *18*, 561.

(27) Boche, G.; Bosold, F.; Lohrenz, J. C. W. *Angew. Chem., Int. Ed. Engl.* **1994**, *33*, 1161.

(28) Jørgensen, K. A. *J. Chem. Soc., Perkin Trans. 2* **1994**, 117.

(29) (a) Fanwick, P. E.; Ogilvy, A. E.; Rothwell, I. P. *Organometallics* **1987**, *6*, 73. (b) LaPointe, R. E.; Wolczanski, P. T.; Mitchell, J. F. *J. Am. Chem. Soc.* **1986**, *108*, 6382. (c) Lubben, T. V.; Wolczanski, P. T.; VanDuyne, G. D. *Organometallics* **1984**, *3*, 977. (d) Coffindaffer, T. W.; Rothwell, I. P.; Huffman, J. C. *Inorg. Chem.* **1983**, *22*, 2906. (e) Chisholm, M. H.; Eichhorn, B. W.; Folting, K.; Huffman, J. C.; Tatz, R. J. *Organometallics* **1986**, *5*, 1599. (f) Bryndza, H. E.; Calabrese, J. C.; Marsi, M.; Roe, D. C.; Tam, W.; Bercaw, J. E. *J. Am. Chem. Soc.* **1986**, *108*, 4805. (g) Rees, W. M.; Churchill, M. R.; Fettinger, J. C.; Atwood, J. D. *Organometallics* **1985**, *4*, 2179.

(30) NBO version 3.1: Glendening, E. D.; Reed, A. E.; Garpenter, J. E.; Weinhold, F.; University of Wisconsin, Madison.

(31) Reed, A. E.; Schleyer, P. v. R. *J. Am. Chem. Soc.* **1991**, *113*, 7363.

(32) O−O: 1.469 Å. (a) Bach, R. D.; Owensby, A. L.; Gorizalez, C.; Schlegel, H. B.; McDouall, J. J. W. *J. Am. Chem. Soc.* **1991**, *113*, 6001. (b) Back, R. D.; Su, M.-D.; Andres, J. L.; Schlegel, H. B. *J. Am. Chem. Soc.* **1993**, *115*, 8763. (c) Boche, G.; Bosold, F.; Lohrenz, J. C. W. *Angew. Chem., Int. Ed. Engl.* **1994**, *33*, 1161.

Table 1. Selected Bond Lengths (Å), Bond Angles (deg), and Dihedral Angles (deg) for Structures **14**–**22**, **25**, and **26** with the BLYP/3-21G Calculations

	14	**15**	**16**	**17**	**18**	**19**	**20**	**21**	**22**	**25**	**26**
					Bond Lengths						
$Ti-O_1$	1.860	1.848	1.859	1.832	1.842	1.880	1.862	1.829	1.839	1.853	1.870
$Ti-O_2$	1.906	1.914	1.905	1.917	1.908	1.907	1.909	1.914	1.909	1.918	1.907
$Ti-O_3$	2.132	2.122	2.112	2.150	2.144	2.140	2.126	2.158	2.149	2.133	2.116
$Ti-O_4$	1.906	2.002	2.005	1.995	2.011	1.980	1.986	1.986	1.988	2.012	2.036
$Ti-O_5$	1.818	1.861	1.856	1.856	1.859	1.847	1.868	1.861	1.878	1.863	1.858
$Ti-O_6$	2.294	2.054	2.056	2.064	2.052	2.049	2.050	2.066	2.058	2.030	2.020
O_4-O_6	1.566	1.807	1.803	1.784	1.793	1.790	1.818	1.789	1.821	1.805	1.800
C_8-C_9	1.339	1.374	1.374	1.373	1.372	1.372	1.375	1.373	1.375	1.372	1.374
C_8-O_4	4.597	2.200	2.184	2.287	2.137	2.257	2.208	2.293	2.166	2.189	2.165
C_9-O_4	4.239	2.056	2.049	2.030	2.148	2.073	2.028	2.031	2.081	2.091	2.078
					Bond Angles						
O_1-Ti-O_2	84.1	84.5	84.9	84.5	84.8	82.6	83.9	84.3	84.5	83.8	83.9
O_1-Ti-O_3	156.3	157.0	156.6	155.4	156.9	155.9	158.4	156.9	157.9	156.6	152.4
O_1-Ti-O_4	102.0	111.4	110.5	116.6	115.5	103.1	101.2	114.2	106.5	115.3	120.1
O_1-Ti-O_6	91.9	97.2	92.4	94.9	90.8	97.0	95.3	95.0	93.5	103.3	95.2
O_2-Ti-O_3	74.0	74.0	74.1	72.1	72.3	75.3	75.1	72.6	73.5	73.1	72.4
O_2-Ti-O_4	136.4	152.8	156.6	154.0	156.9	160.0	157.7	146.3	152.9	151.9	151.3
O_2-Ti-O_6	94.7	104.8	100.5	109.8	104.0	107.9	104.7	100.3	102.0	104.4	114.3
O_3-Ti-O_4	88.2	86.1	85.4	84.3	83.7	94.4	96.7	86.4	94.4	85.5	80.0
O_3-Ti-O_5	91.4	92.9	90.0	99.0	94.7	93.4	93.4	88.7	88.8	90.8	100.4
O_3-Ti-O_6	81.2	81.3	90.0	82.4	91.7	107.9	104.7	100.3	102.0	80.2	82.2
O_5-Ti-O_1	105.7	101.7	99.7	99.6	98.2	103.0	98.4	100.5	98.3	99.8	99.2
O_5-Ti-O_2	113.4	109.7	109.1	114.7	115.7	109.4	110.6	113.8	113.5	109.5	104.8
O_5-Ti-O_4	106.5	89.2	89.3	91.0	88.9	90.5	90.3	91.2	89.9	88.3	87.6
O_5-Ti-O_6	147.9	141.8	142.8	141.9	139.8	139.5	143.2	143.6	143.4	140.6	139.5
$Ti-O_4-O_6$	82.1	65.0	65.1	65.9	65.0	65.6	65.1	66.2	65.2	64.0	63.2
O_4-Ti-O_6	42.5	52.9	52.7	52.0	52.4	52.7	53.5	52.3	53.5	53.0	52.7
					Dihedral Angles						
$O_5-C_7-C_8=C_9$	0.8	−29.8	34.2	−31.2	35.4	−31.7	31.2	−29.3	30.9	−30.0	32.7
$C_7-O_5-Ti-O_4$	108.1	35.8	−37.3	36.4	−37.5	13.9	−47.2	34.1	−48.4	35.9	−33.5
$C_{12}-O_6-O_4-Ti$	−110.5	−114.0	−115.9	120.4	120.5	−115.0	−116.6	121.3	120.2	−127.0	−124.1

conformations, one with the methyl group pointing away from the H_2O moiety (**15** and **16**) and the other with the methyl group pointing toward the H_2O moiety (**17** and **18**). Structures **19**–**22** are derived from structures **15**–**18** by flipping the diolate five-membered ring. All these structures were optimized by the transition state optimization technique with one negative eigenvalue. A frequency calculation on structure **15** with the BLYP/3-21G method showed that it is a true transition structure with one imaginary frequency which corresponds to the motion of oxygen transfer. Although frequency calculations were not carried out for the other structures, based on the similarity in geometries we can safely assume that they are also true transition structures. Selected geometrical parameters and calculated total energies are collected in Tables 1 and 2, respectively.

We also tested whether the accidantal constraint of the $H_1-O_3-Ti-O_2$ and $H_2-O_3-Ti-O_2$ dihedral angles at 7.6° and −169.0° instead of 0° and 180° had serious problems. Starting from the optimized structures of **15** and **16**, the rotation of the two dihedral angles to 0° and 180° caused 0.4 and 0.1 kcal/mol energy rise for the two structures, respectively. Geometric optimizations with the transition structure technique caused almost no changes in geometry and energy (within 0.1 kcal/mol). This suggests that the geometry was not affected by the mistake. The calculated energies of structures **15**, **16**, **19**, and **20** with the 0° and 180° dihedral angles are given in Table 2 (parentheses). Besides structure **15**, these calculated energies are nearly identical to those with the 7.6° and −169° dihedral angles.

(1) Relative Activation Energies. The calculated activation energies of the eight transition structures with respect to the reactant (**14**) are given in Figure 4. In general, the calculated activation energies are lower with the 3-21G basis set but are increased with the HW3 basis set. The lowest activation energy is 12.6 kcal/mol with structure **15**. The activation enthalpy of metal-catalyzed epoxidation has been reported to be 12–15 kcal/mol.[34] The $\Delta H^{\ddagger}$ of 10.2 kcal/mol was reported by Sharpless *et al.* for the epoxidation of (cyclohexenyl)methylcarbinol by TBHP and titanium−(+)-DIPT.[2a] Although the measured $\Delta H^{\ddagger}$ by Sharpless *et al.* includes the equilibrium (K_1K_2) of peroxide and allylic alcohol ($K_{obs} = K_{epox}K_1K_2$, $K_1K_2 \approx 0.7$),[2] our

Table 2. Calculated Total Energies (−au)[a]

	E	
structure	BLYP/3-21G	BLYP/HW3//3-21G
14	1529.94671	746.32600
15	1529.93212	746.30596 (746.30480)[a]
16	1529.93083	746.30527 (746.30528)
17	1529.92616	746.30304
18	1529.92421	746.30046
19	1529.93089	746.30515 (746.30517)
20	1529.93028	746.30520 (749.30536)
21	1529.92399	746.30232
22	1529.92347	746.29994
25	1647.17313	864.17081 (864.16984)
26	1647.17126	864.16787 (864.16722)
27	1755.27085	972.89762
28	1755.26947	972.89678
29	1755.27281	972.89229
30	1755.26990	972.88992

[a] The values in parentheses are the energies with rotation of the H1−O3−Ti−O2 and H2−O3−Ti−O2 dihedral angles to 0° and 180°, respectively.

(33) (a) Schaefer, H. F., III *Acc. Chem. Res.* **1979**, *12*, 288. O−O (expt): 1.475 Å. (b) Jørgensen, K. A.; Swanstrom, P. *Acta Chem. Scand.* **1992**, *46*, 82. O−O(expt): 1.46 Å.

(34) (a) Gould, E. S.; Hiatt, R. R.; Irwin, K. C. *J. Am. Chem. Soc.* **1968**, *90*, 4573. (b) Baker, T. N.; Mains, G. J.; Sheng, M. N.; Zajacek, J. G. *J. Org. Chem.* **1973**, *38*, 1145.

calculated activation energy seems to be in close agreement with the experiment.

There are three notable features in the calculated activation energies. First of all, structures **15**–**18** with the values of 7.6° and −169° for the $H_1-O_3-Ti-O_2$ and $H_2-O_3-Ti-O_2$ dihedral angles are all slightly more stable than structures **19**–**22**, which differ only in the five-membered diolate ring puckering. With the values of 0° and 180° for the two dihedral angles, structures **15**, **16**, **19**, and **20** are nearly identical in stability. This indicates that there is no significant preference for either top or bottom loading of allylic alcohol in the absence of steric interactions.

Secondly, there is a preference for the methyl group of the peroxide to be directed away from the water ligand instead of toward it. For example, at the HW3 basis set level, structure **15** is 1.8 kcal/mol more stable than structure **17** and structure **16** is 3.3 kcal/mol more stable than structure **18**. Similar situations are found for structures **19**–**22**. We believe that this conformational preference is primarily due to electrostatic interactions. The OMe group in **15** is oriented in such a way that its lone pair electrons can point to the water moiety. The water oxygen is slightly positively charged due to electron donation into titanium (+0.16). On the other hand, the OMe lone pair in structure **17** directs toward the diolate O_1, which is much more negatively charged (−0.67). Therefore, structure **17** is destabilized by electrostatic repulsion. This effect of electrostatic interaction is also evident from the basis set dependence of the energies. For each pair of transition structures, the 3-21G basis set gives a larger energy difference because the 3-21G basis set is known to overestimate the electrostatic interaction. Steric interaction between the methyl and the water also contributes to the destabilization of **17**, **18**, **21**, and **22**.

Finally, the allyl moiety has no conformational preference when the methyl group of the peroxide directs away from the bridging H_2O (**15**, **16**, **19**, **20**). When the methyl group of the peroxide directs toward the bridging H_2O, a large preference of about 1.5 kcal/mol is found for structures **17** and **21** over structures **18** and **22**, respectively.

It is interesting that the calculated activation energy with structure **15** is only about 2 kcal/mol higher than that of a monomeric model (**9**) where the sixth water ligand is absent. This gives strong support to the Sharpless dimeric mechanism of titanium tartrate catalyzed epoxidation. It has been shown that the Sharpless reagent titanium tartrate exists predominantly as a dimer in solution.[13] The NMR spectra indicate that at room temperature there is a fluxional process that renders the two halves of the tartrate molecule equivalent. The activation barrier of this site exchange process is about 12−15 kcal/mol.[13] If the reaction takes place via the monomeric pentacoordination transition state, it has to overcome the dissociation energy first. Recent work by Erker *et al.* with catecholato−zirconocene complexes indicates that the dissociation energy from dimer to monomer is even higher than the barrier to the internal fluxional.[11] Thus, the activation energy for the monomeric mechanism would be much higher than the dimeric mechanism when the dissociation energy is included.

(2) Geometries. Structures **23** and **24** are the stereoviews of the optimized structures **15** and **16**, respectively. Other structures are not displayed, but the selected geometrical parameters are collected in Table 1. These transition structures are quite similar in terms of the forming epoxide unit and the structure about the Ti center. In each structure, the C=C double bond approaches the Ti−O−OMe in a nearly spiro fashion with the C=C nearly anti to the breaking O_4-O_6 bond, as can be clearly seen from structures **23** and **24**. This is the same as in structures **8** and **9**. A molecular orbital explanation for the spiro preference has been described before.[18] We were unable to locate a planar transition structure. The inner forming C−O bond is about 0.1−0.2 Å longer than the outer forming C−O bond in every structure except for structure **20** in which the two bond lengths are about the same.[35] This nearly symmetrical transition structure is in agreement with the experimental observation by Sharpless *et al.* that the secondary deuterium isotope effects at the C_2 and C_3 of allylic alcohol are very similar. They also reached the conclusion that the external C−O bond is formed to a slightly greater extent.[13] The slightly longer length of the inner C_8-O_4 bond is probably due to torsional rather than electronic factors.

In each of the structures, the $Ti-O_6$ bond is only slightly longer than the $Ti-O_4$ bond. Thus, the Ti−O−O(Me) has a good η^2 structure. Overall, these transition structures can be regarded as distorted octahedrons, mainly due to two small O−Ti−O angles: one is the O_2-Ti-O_3 angle which is 72.1°−75.3° in the eight structures; the other is the O_4-Ti-O_6 angle which ranges from 52.0 to 53.5°. In every structure, $Ti-O_1$ is shorter than $Ti-O_2$. This is mainly because the $Ti-O_1$ bond is anti to the weaker donor OH_2, as indicated by the longest $Ti-O_3$ bond length, while $Ti-O_2$ is anti to a stronger donor O_4.

While the O_1-Ti-O_2 and O_2-Ti-O_3 angles are nearly constant, several other O−Ti−O angles vary quite substantially. In particular, the O_1-Ti-O_4 angles are considerably larger than the O_3-Ti-O_4 angles. This most likely results from the weaker $Ti-O_3$ bond (when compared with $Ti-O_1$) because it is also true in the reactant (**14**). Interestingly, the two angles are dependent upon the orientation of the peroxy methoxy group. Thus, the O_1-Ti-O_4 angle increases by 4−11° when the methoxy group changes from anti to the OH_2 (e.g. **15**) to syn to the OH_2 (e.g. **17**). Simultaneously, the O_3-Ti-O_4 angle becomes smaller by 2−8°. The simplest explanation for this would be based on electrostatic interaction. The attractive interaction between the metal center and the lone pair on O_6 in structure **17** forces the O_1-Ti-O_4 angle to open up.

Ring flipping also causes conformational changes. The most significant change is in the O_3-Ti-O_6 angle. The angle ranges from 81 to 92° in structures **15**–**18**. After flipping of the five-membered diolate ring, the angle increases to 100−108° in structures **19**–**22**.

The $O_5-C_7-C_8=C_9$ dihedral angle ranges from 29.3 to 35.4°. According to Houk's definition, these are "inside" oxygen transition structures.[36] The $C_7-O_5-Ti-O_4$ dihedral angle is quite small (14°) in structure **19**, but becomes larger in the other structures. The $C_{12}-O_6-O_4-Ti$ dihedral angle also increases from 111° in the reactant to 114−120° (in absolute value) in the transition structures. This reflects the increased $Ti-O_6$ bonding and decreased O_4-O_6 bonding in the transition structures.

C. Effect of *tert*-butyl Hydroperoxide. To understand the effect of the bulkiness of alkyl peroxide on the transition structures and therefore stereochemistry, the methyl group in

(35) For related epoxidation transition structures, see: (a) Bach, R. D.; Mcdouall, J. J. W.; Owensby, A. L.; Schlegel, H. B. *J. Am. Chem. Soc.* **1990**, *112*, 7065. (b) Back, R. D.; Coddens, B. A.; McDouall, J. J. W.; Schlegel, H. B.; David, F. A. *J. Org. Chem.* **1990**, *55*, 3325. (c) Bach, R. D.; Owensby, A. L.; Gonzalez, C.; Schlegel, H. B.; McDouall, J. J. W. *J. Am. Chem. Soc.* **1991**, *113*, 2338. (d) Bach, R. D.; Owensby, A. L.; Gonzalez, C.; Schlegel, H. B.; McDouall, J. J. W. *J. Am. Chem. Soc.* **1991**, *113*, 6001. (e) Bach, R. D.; Andrés, J. L.; Davis, F. A. *J. Org. Chem.* **1992**, *57*, 613.

(36) Houk, K. N.; Moses, S. R.; Wu, Y.-D.; Rondan, R. G.; Jager, B.; Schohe, R.; Fronczek, F. R. *J. Am. Chem. Soc.* **1984**, *106*, 3880.

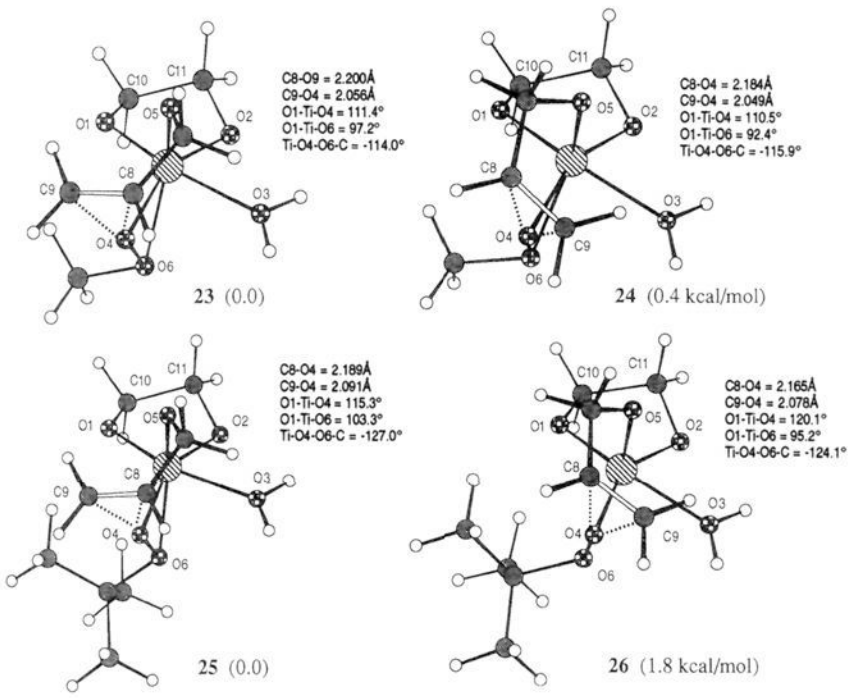

Figure 5. Stereoviews of the optimized transition structures with methyl peroxide as the oxidant (**23** and **24**) and with *tert*-butyl peroxide as the oxidant (**25** and **26**). Calculated relative energies are in parentheses.

structures **23** and **24** was replaced by a *tert*-butyl group. Full geometrical optimizations were carried out for the two transition structures. The stereoviews of the two structures are given in Figure 5 along with some selected geometrical parameters. More detailed geometrical parameters are found in Table 1.

Overall, the bulky *tert*-butyl group causes only minor changes in bond lengths. However, it causes geometrical changes in the Ti−O_4−O_6−R unit. The Ti−O_4−O_6−C dihedral angle in structures **25** and **26** is 127° and 124°, respectively, compared to 114° and 116° in structures **23** and **24**. Accompanying these changes in the dihedral angle is the widening of the O_1−Ti−O_4 and O_1−Ti−O_6 angles. These geometrical changes are undoubtedly due to the steric interactions between the *tert*-butyl group and the diolate ring. When the three methyl hydrogens in structure **23** were replaced by three standard methyl groups (C−C = 1.54 Å, C−H = 1.09 Å, and C−C−H = 109.5°), one of the *tert*-butyl hydrogens was only 1.45 Å away from O_1, and another *tert*-butyl hydrogen was separated from the axial hydrogen at C_{10} by 1.817 Å. In the optimized structure **25**, these two distances became 2.219 and 2.313 Å, respectively. The same steric effects occur in structure **26**.

It is most interesting that the calculated preference for structure **25** over structure **26** is 1.8 kcal/mol compared to 0.4 kcal/mol for structure **23** over structure **24**.[37] Since the methyl and *tert*-butyl have similar electronic effects, we attribute the large variation in the allyl conformational preference to steric effect. As discussed above, the steric effect of the *tert*-butyl group opens up the O_1−Ti−O_4 and O_1−Ti−O_6 angles. In the case of methyl peroxide, the allyl conformational preference is small when the peroxide methyl is away from the water ligand (e.g. structures **15** and **16**) but is larger when the methyl directs to the water ligand (e.g. structures **17** and **18**). We note that the O_1−Ti−O_4 angle increases by 5−9° but the O_1−Ti−O_6 angle decreases only by about 2° when the methyl is switched from away from the water ligand to directing toward the water ligand. It might be possible that the allyl conformational preference is correlated with the opening of the O_1−Ti−O_4 and O_1−Ti−O_6 angles.

D. Tartrate Ester Groups. Another important factor to consider is the conformation of the tartrate ester groups in the transition structures of epoxidation. Would they favor axial positions or equatorial positions? What would be the steric and electronic interactions of these groups with the allyl moiety? To answer these questions, we selected transition structures **15** (**23**) and **16** (**24**) as representatives since they are the most stable transition state pair that lead to two enantiomers.

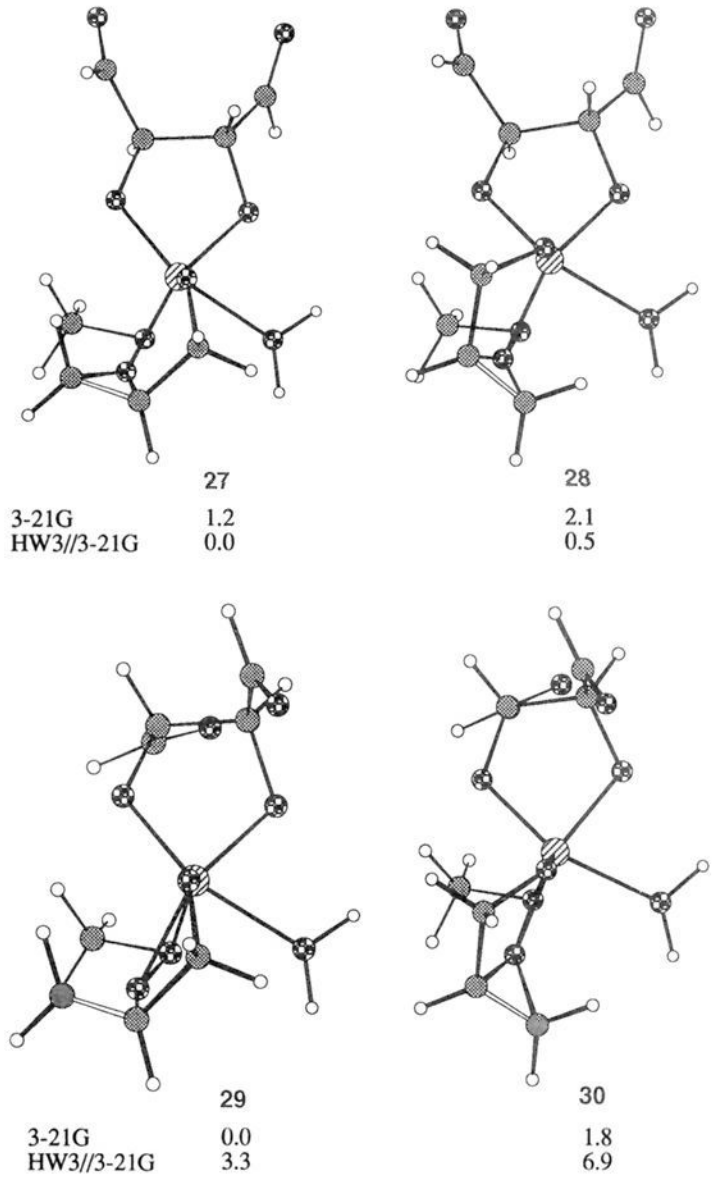

Figure 6. Stereoviews of diequatorial and diaxial formyl substituted transition structures derived from structures **23** and **24**, respectively. Only the formyl groups are optimized. The calculated relative energies are in kcal/mol.

We used formyl groups to mimic the ester groups mainly for computational convenience. Jørgensen *et al.* also used formyl groups to replace the ester groups in their earlier modeling of the reaction.[16] Four structures can be derived based on structures **15** and **16**. As shown in Figure 6, structures **27** and **28** have the formyl groups in the equatorial positions in the five-membered diolate ring, whereas structures **29** and **30** have the formyl groups in the axial positions. These structures were optimized with the 3-21G basis set by fixing all atoms except for the formyl groups. The energetics of these structures were also calculated with the HW3 basis set.

In the two equatorial structures **27** and **28**, the formyl groups are in similar conformations. The C=O bonds are nearly anti to the diolate C−O bonds with O−C−C=O dihedral angles of about 150°. Since these formyl groups have essentially no steric interaction with both the allyl moiety and the alkyl peroxide, it is not surprising that the calculated preference for structure **27** over structure **28** (0.5 kcal/mol with the HW3 basis set) is almost identical to that for structure **15** over structure **16** (0.4 kcal/mol with the HW3 basis set).

In the two axial structures **29** and **30**, the C=O group which lays on the side of the allylic alcohol moiety nearly eclipses the C−O2 diolate bond while the other C=O nearly eclipses the C−C bond.[38] There is no involvement of the carbonyl oxygen in metal coordination, as indicated by large Ti/O

(37) With the values of 0° and 180° for the H1−O3−Ti−O2 and H2−O3−Ti−O2 dihedral angles, structure **24** is more stable than **23** by 0.3 kcal/mol, but structure **25** is still more stable than **26** by 1.6 kcal/mol (see Table 2).

distances (larger than 3.6 Å). This is in agreement with a qualitative analysis by Sharpless *et al.*[2a,7a] This is expected because the six coordination sites of titanium have already been occupied.

The calculated relative energies of these structures are quite basis set dependent. When the 3-21G basis set is employed, structure **29** appears to be the most stable and structure **28** is least stable (2.1 kcal/mol). At the HW3 level, however, the two equatorial structures become much more stable than the two axial structures. Thus, structures **29** and **30** are respectively 3.3 and 6.9 kcal/mol less stable than structure **27**. The large basis set dependence of the energetics is expected because electrostatic interaction is significantly involved, and the 3-21G basis set does not give a satisfactory description of electrostatic interaction. The HW3 which contains polarization functions, should give much more reliable results.[39] It needs to be noted that solvent effect may also significantly influence the relative energies.[40] At this point, we think that the axial formyl groups cause destabilization both for steric and electrostatic reasons. The distance between the formyl oxygen and the allylic oxygen is 3.209 Å in **29** and 3.197 Å in **30**, and electrostatic repulsion between the two oxygen atoms should be significant. It is also worth mentioning that, besides this O/O repulsion, there should be no significant steric interaction between the formyl and allyl groups. This means that the enantioselectivity of the epoxidation process is unlikely caused by steric effects of the ester groups on the reactive titanium center and the allyl moiety.

In support of the equatorial conformational preference of tartrate ester groups in the epoxidation transition structure, we note that the X-ray crystal structures of metal tartrate complexes do indicate the equatorial conformation of esters when they are not involved in coordination with the metal. For example, in the titanium tartrate hydroxamate complex,[12a] since the axial coordination site is occupied by the hydroxamate ligand, coordination occurs between the titanium and tartrate ester carbonyl oxygen. Therefore, the tartrate ester groups occupy the equatorial positions. This situation is also found in the X-ray crystal structure of the tartrate–ziconocene complex.[11b] Therefore, it is likely that in the Sharpless epoxidation, there is a conformational change in the five-membered diolate ring, while in the reactant, the ester groups have to take the axial positions in order for the tartrate ester to achieve coordination with the titanium atom. However, ring flipping should occur during formation of the epoxide transition state. The consequence of this conformational feature will be discussed in more detail later.

E. The Dimeric Transition Structure Model. The results discussed above can be summarized as follows: (1) Epoxidation transition structure favors a spiro geometry instead of a planar geometry. (2) There is a significant preference for the alkyl group of the alkyl peroxide to orient away from the H_2O moiety in order to enhance electrostatic attraction and to minimize steric interaction. (3) There is a large preference for the allylic alcohol moiety to adopt the conformation in which the C–O bond bisects the Ti–O bonds of the H_2O moiety and the peroxygen

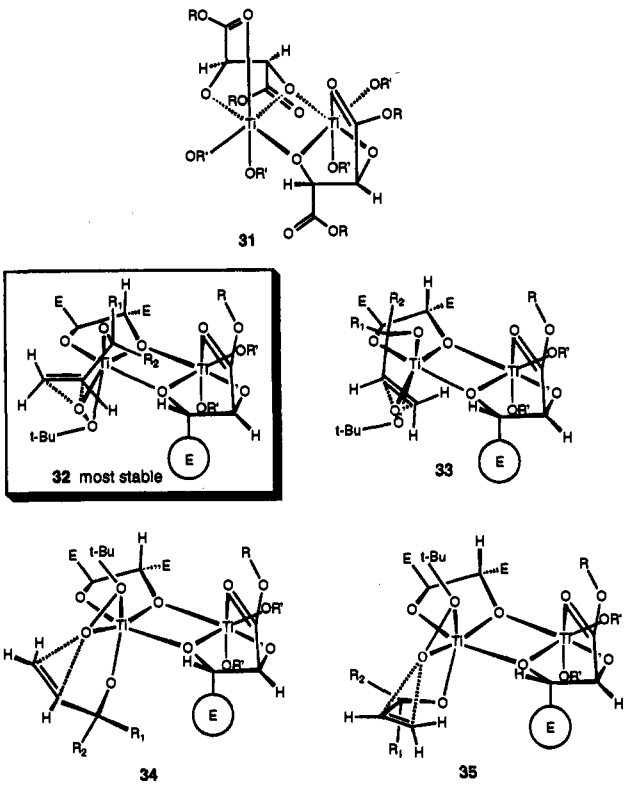

Figure 7. The dimeric structure of Ti(tartrate)(OR)2 (**31**) and four spiro transition structures (**32**–**35**) of the modified Sharpless dimeric model.

when the oxidant is bulky *tert*-butyl hydroperoxide. This conformational preference vanishes with methyl hydroperoxide as the oxidant. (4) The tartrate ester groups in the epoxidation transition structure are not involved in coordination with titanium and they prefer the equatorial conformation instead of the axial conformation as in the dimeric titanium tartrate complex.

Based on these results we develop a modified Sharpless dimeric model to explain the stereoselectivity of the Sharpless epoxidation. We use L-(+)-tartrate as an example. The reactive catalyst is in a dimeric form as shown by structure **31**. This leads to four spiro transition structures **32**–**35**.[41] Structures **32** and **33** have the allylic alcohol loaded on the top and are derived from structures **15** and **16**, respectively. Structures **34** and **35** have the allylic alcohol loaded on the bottom and are derived from the mirror image of structures **19** and **20**, respectively.

The key features of the transition structure model and the explanation for stereochemistry are discussed as follows:

(1) Diolate Ring Flipping. The ester groups on the reactive titanium center are arranged in equatorial conformation. Since the two ester groups are in the axial conformation in the reactant (**31**), there is a diolate ring flipping upon the formation of transition structure. Although this feature was not proposed in their original paper, Sharpless *et al.* implicated it in a recent publication.[4] It is found that 1:1 Ti–**36** catalyst essentially showed no reactivity in the epoxidation under normal reaction conditions. The reaction occurs at elevated temperatures, but with total loss of stereoselectivity.[4] Sharpless *et al.* attributed this phenomenon to the prevention of the formation of η^2-alkyl peroxide binding, thus shutting down the complex's reactivity. This is similar to our idea that the presence of the cyclohexane ring locks the two ester groups in the axial positions which causes a higher energy transition structure.

(38) Based on extended Hückel molecular orbital calculations, Jørgensen *et al.* found that the formyl groups orient in such a way that the C=O is eclipsed with the C–C bond. They suggested that this might enhance the orbital overlap between the oxygen π orbital of the allylic alcohol and the π^* orbital of the C=O bond (see ref 16). This feature is not found in our calculations. In both structures **29** and **30**, the formyl group on the side of allyl moiety eclipses with the C_{11}–O_2 bond. Besides, the distance between the oxygen atom of the allylic alcohol and the carbonyl carbon is 3.693 Å and 3.675 Å in structures **29** and **30**, respectively. Such large separation cannot achieve an effective orbital overlap.

(39) Hehre, W. J.; Radom, L.; Schleyer, P. v. R. *Ab Initio Molecular Orbital Theory*; Wiley-Interscience: New York, 1986.

(40) Wong, M. W.; Frisch, M. J.; Wiberg, K. B. *J. Am. Chem. Soc.* **1991**, *113*, 4776.

(41) These structures were built by the replacement of the water molecule in the optimized model transition structures with the bystander titanium center. No geometric refinement was carried out.

(2) Peroxide Conformation. The *tert*-Bu of the peroxide orients away from the bridging oxygen in every structure. The model calculations suggest that if the *tert*-butyl group directs toward the bridging oxygen it will suffer from significant steric interactions with the diolate on the bystander titanium center. In the original Sharpless model, the *tert*-butyl group directs toward the bridging oxygen because it has to avoid steric interaction with the axial ester group. With the equatorial ester groups in the current model, this steric effect is absent.

(3) Steric Effect of Ligand. If steric effect were absent, according to the earlier model calculations, structures **32** and **34** would be more stable than structures **33** and **35**, respectively, since the former have the allylic C−O bond gauche to the Ti−$O_{bridging}$ bond. In structures **32** and **33**, the allylic alcohol is loaded on the top, and it has no steric interaction with the non-coordinating ester group (circled) of the bystander center.[42] However, structures **34** and **35** have the allyl and the ester groups on the same side, and suffer from some steric interactions. This is especially severe in structure **34**. To appreciate this, we placed a methyl at the circled E, and found that one of the methyl hydrogens was about 1.5 Å away from the allylic hydrogen at the R1 position (R1 = H). Indeed, this steric effect is crucial to high enantioselectivity. In the absence of this group, transition structures **32** and **34** should have similar stabilities since both structures do not suffer from steric interactions, and the relative stabilities of the two structures should be similar to those of structures **15** and **19**. This is in accord with the low enantioselectivity in entry 6 in Figure 1. The presence of the ester group, which can be replaced by an alkyl group (see entries 1, 4, and 5 in Figure 1), significantly destabilizes structure **34** and results in high enantioselectivity.

(4) Effect of Bulky Peroxide. While the effect of a bulky alkyl group on enantioselectivity is intriguing, the phenomenon has not been explained satisfactorily in the literature. Sharpless *et al.* suggested that when *n*-butyl peroxide is used instead of t-butyl peroxide, the primary alkyl group has access to different orientations,[6] for example, both toward and away from the bridging oxygen. This could result in a lower enantioselectivity. Our model provides a unique explanation for this intriguing phenomenon. We suggest that structure **32** is most stable and is most responsible for the formation of the major enantiomer.[43] Structure **33** is responsible for the formation of the minor enantiomer. The energy difference between structures **32** and **33** reflects the energy difference between structures **25** and **26**, which leads to high enantioselectivity. When the *tert*-butyl peroxide is replaced by a primary alkyl peroxide, the energy difference reflects that between structures **15** and **16**, and a low enantioselectivity is expected.

(5) Spiro versus Planar TS. We prefer an all spiro transition structure model instead of a planar transition structure for the formation of the minor epoxy alcohol enantiomer as in the original Sharpless model[2a] for the following two reasons. (1) Model calculations indicate that a planar transition structure is about 3 kcal/mol less stable than a spiro transition structure,[18] and this energy difference is too large to account for the observed enantioselectivity. (2) The all spiro transition structure model better accounts for the tolerance of high levels of asymmetric induction toward wide variation in allylic alcohol structure. The spiro transition structures have the allylic C−O bond in an "inside" position with a dihedral angle of C=C−C−O about 30° as shown by **37** and **38** which are the Newman

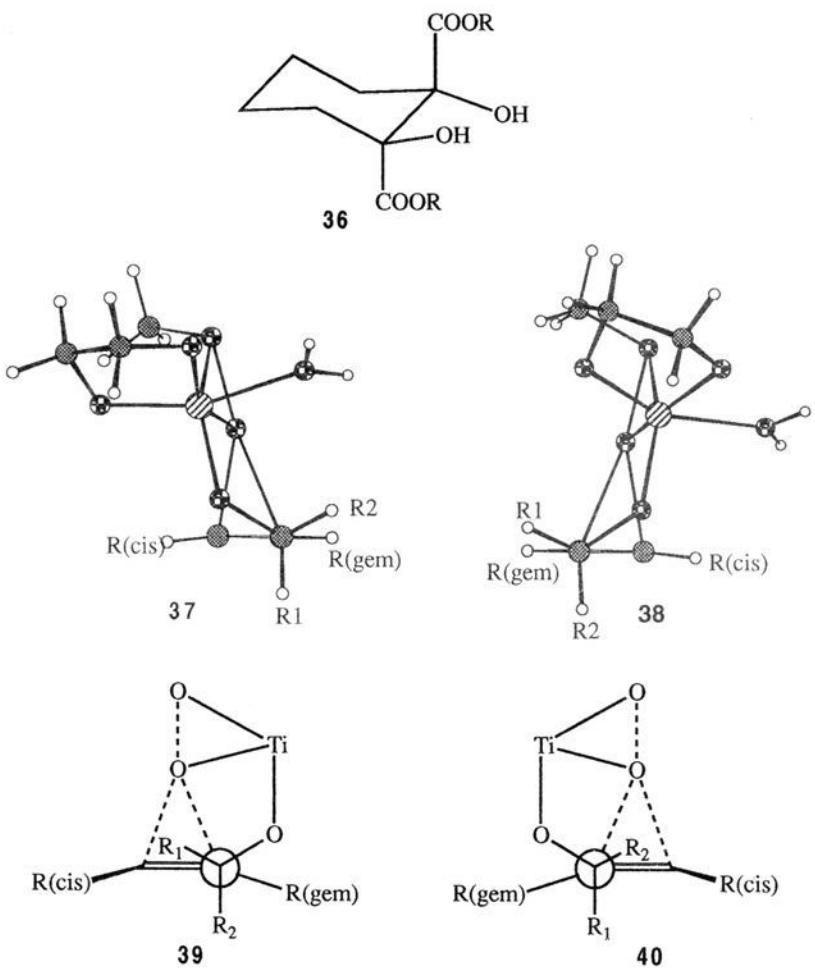

projections of structures **23** and **24** along the C_8−C_7 bond. A planar transition structure would require a C=C−C−O dihedral angle of about 150° for the allylic moiety, and the C−O bond would be in the "outside position" as shown by Newman projections **39** and **40**. When a cis substituent is present, it causes considerable destabilization to spiro transition structures. This is in accord with the fact that cis allylic alcohols undergo the Sharpless epoxidation with reduced reactivity. On the other hand, a cis alkyl group can only have a small effect on a planar transition structure. A geminal alkyl group (on C_2 of allylic alcohol) would destabilize a planar transition structure but have little effect on a spiro transition structure. If a planar transition structure (**40**) is responsible for the formation of the minor enantiomeric product, it would be expected that a cis substituent significantly reduces enantioselectivity while a geminal substituent increases enantioselectivity. Experimentally, a geminal group has little influence on enantioselectivity while a primary cis substituent also causes little reduction in enantioselectivity.[2] These are expected by the all spiro transition structure model (**37** and **38**).

(6) Diastereoselectivity. Finally, the model explains observed diastereoselectivity and kinetic resolution. When the allylic alcohol is chiral (either R1 or R2 is alkyl), the enantiomeric allylic alcohol with R1=alkyl should be more reactive because the R1 position in transition structure **32** is uncrowded but the R2 position is very crowded. Since in transition structure **33** the reverse is true, it is expected that the diastereoselectivity is high for the more reactive enantiomeric allylic alcohol but low for the less reactive alcohol if the allylic alcohol has no cis substituent. On the other hand, when the alcohol is cis substituted, the diastereoselectivity for the more reactive enantiomeric alcohol (R1 = alkyl) is expected to be low or even reversed because,[3b] as can be seen in structure **37**, the cis alkyl substituent causes significant destabilization to structure **32** but has much less effect on structure **33** because the R1 in structure **33** is away from the cis substituent (see structure **38**).

(42) Recently Jørgensen reported a force-field modeling of the enantioselectivity of titanium tartrate catalyzed oxidation of sulfides based on ab initio calculations and X-ray structures of titanium tartrate complexes. Steric effect was shown to be important for the enantioselectivity (see ref 28).

(43) The transition structure for the major product in the original Sharpless model corresponds to structure **35**. A rotation of 180° about the axis through the two bridging oxygen atoms is needed to convert that structure into the current view.

F. Summary. Non-local density functional calculations (BLYP) have been carried out on a hexacoordinate monomeric model of the Sharpless epoxidation. Detailed conformational features of the epoxidation transition structures have been obtained. The Ti−O−O(R) unit is in a η^2 structure. The approach of the Ti−O−O to the allyl C=C bond is in a spiro fashion. The outer C−O forming bond is about 0.1−0.2 Å shorter than the inner C−O forming bond. This agrees with the secondary isotope effect on epoxidation observed by Sharpless *et al.*

The allyl moiety strongly prefers to be gauche to the Ti−$O_{bridging}$ and the Ti−$O_{peroxygen}$ bond when the oxidant is *tert*-butyl peroxide. The conformational preference vanishes for methyl peroxide. This conformational feature is likely caused by the larger steric interaction between the peroxide alkyl group and the diolate when the allylic C−O bond is gauche to the end Ti−O diolate bond. We suggest that this is associated with the requirement of a bulky alkyl peroxide for high enantioselectivity.

In agreement with the earlier assessment by Sharpless *et al.* the ester groups on the reactive titanium center are not involved in coordination with titanium in the transition structure of epoxidation. Since the ester groups favor the equatorial positions instead of the axial positions in the transition structures, we propose that a ring flipping of the five-membered diolate ring occurs during the formation of the epoxidation transition structure.

The Sharpless dimeric model is modified based on the model calculations to better account for the experimentally observed stereoselectivities. The advantage of an all spiro transition structure model is discussed. The model accounts for the importance of the bulky peroxide and ligand structure to the enantioselectivity.

Acknowledgment. We are grateful to Professor K. N. Houk (University of California, Los Angeles) for helpful suggestions. We especially thank Professor Paul Carlier (HKUST) for the many discussions and comments on the subject. Financial support from Hong Kong RGC (HKUST 215/93E) and HKUST (RI93/94.SC03) are acknowledged. We also thank CCST of HKUST for providing valuable computing facilities.

JA9501124